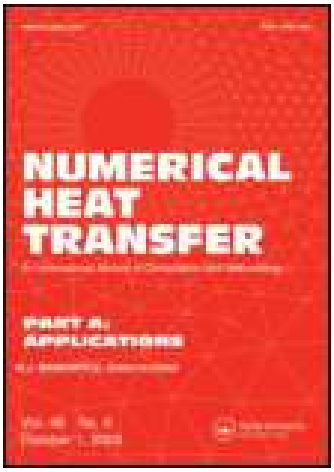

Numerical Heat Transfer, Part A: Applications: An International Journal of Computation and Methodology
Publication details, including instructions for authors and subscription information:
http://www.tandfonline.com/loi/unht20

Three-Dimensional Natural Convection in the Horizontal Bridgman Configuration Under Various Wall Electrical Conductivity and Magnetic Field

Mouna Battira [a] & Rachid Bessaïh [a]
[a] LEAP Laboratory, Department of Mechanical Engineering, Faculty of Engineering , University of Mentouri-Constantine , Constantine, Algeria
Published online: 22 Dec 2008.

To cite this article: Mouna Battira & Rachid Bessaïh (2008) Three-Dimensional Natural Convection in the Horizontal Bridgman Configuration Under Various Wall Electrical Conductivity and Magnetic Field, Numerical Heat Transfer, Part A: Applications: An International Journal of Computation and Methodology, 55:1, 58-76, DOI: 10.1080/10407780802603113

To link to this article: http://dx.doi.org/10.1080/10407780802603113

Numerical Heat Transfer, Part A, 55: 58–76, 2009

ISSN: 1040-7782 print/1521-0634 online
DOI: 10.1080/10407780802603113

THREE-DIMENSIONAL NATURAL CONVECTION IN THE HORIZONTAL BRIDGMAN CONFIGURATION UNDER VARIOUS WALL ELECTRICAL CONDUCTIVITY AND MAGNETIC FIELD

Mouna Battira and Rachid Bessaïh
LEAP Laboratory, Department of Mechanical Engineering, Faculty of Engineering, University of Mentouri-Constantine, Constantine, Algeria

A numerical investigation of the three-dimensional natural convection of a liquid metal contained in the horizontal Bridgman configuration, having an aspect ratio equal to 5 and submitted to an external magnetic field in either the longitudinal or vertical direction, is presented. The numerical approach is based on the finite-volume approximation. A computer program based on the SIMPLER algorithm is developed. The effect of a magnetic field provides a notable change on the flow and thermal structures. The strongest stabilization of the convection flow is found when the magnetic field is oriented vertically. Also, wall electrical conductivity has an effect on the average Nusselt number. A good agreement between our numerical simulations and experimental data found in the literature is obtained.

1. INTRODUCTION

Natural convection in enclosures containing liquid metals has various engineering applications such as materials processing, crystal growth, cooling systems for nuclear reactors, etc. During the crystal growth by the horizontal Bridgman technique (Figure 1), sufficiently high variations in temperature can occur in the melt bath, which generate significant movements by convection within the fluid. Because of the appearance of striations which can affect the growth rate and structure of the solid and thus its quality, the application of a magnetic field is recognized on the flow stability.

For example, Tagawa and Ozoe [1] carried out a numerical study of three-dimensional natural convection of a liquid metal in a cubical enclosure, in the presence of an external magnetic field, applied parallel to the heated and cooled walls. They clarified the theoretical basis for the enhancement of heat transfer under a static magnetic field. Benhadid and Henry [2] studied numerically the natural convection in a parallelepiped cavity for highly conducting fluid under the uniform

Received 1 July 2008; accepted 22 October 2008.

The authors gratefully acknowledge the financial support of this work (doctorate thesis) through project N° J2501/03/57/06 provided by the Algerian Ministry of High Education and Scientific Research. The authors also take this opportunity to express sincere respect to the reviewers for theirs comments.

Address correspondence to Mouna Battira, LEAP Laboratory, Department of Mechanical Engineering, Faculty of Engineering, University of Mentouri-Constantine, Route de Ain El. Bey, Constantine 25000, Algeria. E-mail: mounamaache@yahoo.fr

NOMENCLATURE

A	aspect ratio ($=L/H$) [-]
$\vec{B}$	dimensionless magnetic flux density vector [-]
B_0	uniform magnetic flux density, T
$\vec{g}$	acceleration due to gravity, m/s^2
Gr	Grashof number ($=g\beta(T_h - T_c)L^3/\nu^2$)
$\vec{e}_B$	unitary vector of the direction of $\vec{B}$
H	height of the enclosure, m
Ha	Hartmann number ($=B_0L\sqrt{\sigma/\mu}$)
$\vec{j}$	electric current density, A/m^2
k	thermal conductivity of the fluid, $W/m \cdot K$
L	length of the enclosure, m
Nu	local Nusselt number [-]
Nu_{avg}	average Nusselt number [-]
p	dimensionless pressure [-]
Pr	Prandtl number ($=\nu/\alpha$)
T	dimensionless temperature [-]
T	ambient temperature, K
t	dimensionless time [-]
$\vec{V}$	dimensionless velocity vector [-]
u, v, w	dimensionless velocities in x-, y-, and z-directions, respectively [-]
W	width of the enclosure, m
x, y, z	dimensionless longitudinal, vertical, and transversal coordinates, respectively [-]
α	thermal diffusivity of the fluid, m^2/s
β	thermal expansion coefficient of the fluid, K^{-1}
μ	dynamic viscosity of the fluid, $Pa \cdot s$
ν	kinematic viscosity of the fluid, m^2/s
ρ	density of the fluid, kg/m^3
σ	electric conductivity, $\Omega^{-1} \cdot m^{-1}$
φ	electric potential, V

Subscripts

c	cold
h	hot
0	ambient

magnetic field. They showed that the flow evolution depends on the direction and the intensity of the magnetic field. Emery and Lee [3] simulated the natural convection in a square enclosure with heated vertical walls and temperature-dependent conductivity and viscosity for Prandtl numbers ranging from 0.01 to 1.0, which is representative of liquid metals and gases, and $Ra \leq 10^6$. The overall heat transfer was found to be unaffected and was accurately correlated in terms of the Rayleigh and Prandtl numbers. This correlation applies to both isothermal and constant heat flux hot walls. Bessaih et al. [4] investigated numerically the combined effect of wall electrical conductivity and direction of the magnetic field on the buoyancy-induced flow of gallium in a cubical enclosure. Their results indicate that one can control the flow

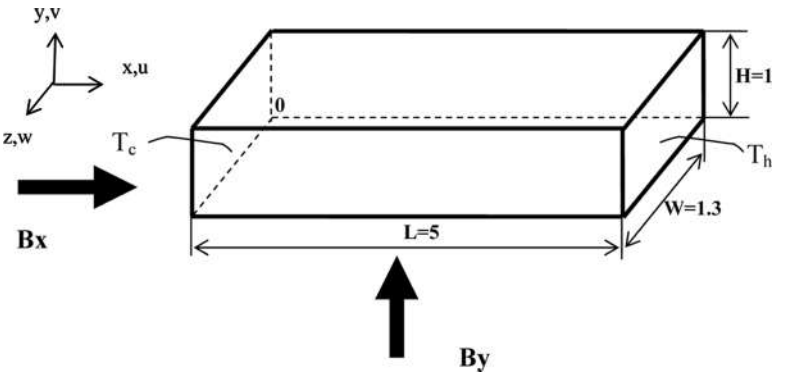

Figure 1. Geometry of problem. The left and right walls are maintained at T_c and T_h, respectively, and the others walls are adiabatic. Bx and By denote the longitudinal and the vertical magnetic field, respectively.

via a good choice of the strength and direction of the magnetic field, as well as of the electric conductivity of the cavity walls. Saravanan and Kandaswamy [5] studied the effect of temperature-dependent thermal conductivity on the buoyancy-induced convection in low-Prandtl-number fluids contained in a square cavity. In absence of a magnetic field, they found that an increase in thermal conductivity reduces both conductive and convective modes of heat transfer. In the presence of a vertical magnetic field, this increase in thermal conductivity produced a highly damped convection and conduction. Arcidiacono et al. [6] and [7] presented a direct numerical simulation for the free convection flow of a low-Prandtl number fluid with internal generation in a slender enclosure ($A = 4$) [6], and in a shallow cavity ($A = 0.25$) [7], having adiabatic top and bottom walls, and isothermal side walls. They determine the Grashof range for which the flow is steady, time-periodic, or chaotic. Aleksandrova and Molokov [8] constructed an asymptotic model of a three-dimensional convection in a rectangular box with electrically insulating walls, and with an horizontal temperature gradient in a strong magnetic field. Their convective heat transfer analysis for low values of the Peclet number shows that either the vertical or the longitudinal magnetic field is the most efficient in damping of the convective heat transfer, depending on the dimensions of the cavity.

Krakov and Nikiforov [9] studied numerically the influence of a uniform magnetic field on the natural convection in a square cavity. They found that the angle between the directions of temperature gradient and magnetic field influences the convection structure. Later, by another numerical simulation and physical experiment [10], they numerically discovered that a set of numerous convective structures exists in the cube, and the structure that is more stable depends on the comparison of magnetic and gravity forces. Experimentally, they found an essential dependence of heat flux on magnetic fields both in vertical and horizontal magnetic fields. Sarris et al. [11] presented a numerical study of unsteady two-dimensional natural convection of an electrically conducting fluid in a laterally and volumetrically heated square cavity under a magnetic field. The flow is characterized by the external Rayleigh number Ra_E, the internal Rayleigh number, Ra_I, and the Hartmann number Ha. They concluded that the flow oscillations were reduced or vanished for increased Ha numbers due to the magnetic field damping effect, but not analogous to the increase of the ratio $S = \mathrm{Ra}_I/\mathrm{Ra}_E$. The heat transfer is enhanced with increasing S, but no significant effect of the magnetic field was observed due to the small range of the Ha numbers studied. Sophy et al. [12] numerically examined the gradient magnetic field influence on the natural convection in a differentially heated square cavity for Rayleigh numbers ranging from 10^3 to 10^5. They showed that a great modification of the flow pattern occurs when the maximum value of the magnetic field is beyond a critical one. Kaneda et al. [13] presented both experimentally and numerically the study of natural convection of liquid gallium under a uniform magnetic field with an external electric current. They found that the magnetic field suppresses the convection, but the interaction of the magnetic field and the additional electric current induces the Lorentz force and it affects the flow pattern and the heat transfer rate from the hot wall to the cold wall, depending on the combination of the external electric current and the direction of the magnetic field.

In the work of Hof et al. [14] and [15], an experimental study of magnetohydrodynamic damping of sidewall convection in a rectangular enclosure filled with

gallium was conducted. The authors investigate the suppression of convection when a steady magnetic field is applied separately in each of the three principal directions of the flow. The strongest damping of the steady flow is found for a vertical magnetic field. However, they observed that the application of a transverse field provides greater damping than a longitudinal one. Xu et al. [16] presented an experimental investigation on natural convection in a gallium contained in a rectangular box with the two opposite vertical walls held at different temperatures. The imposed magnetic fields are parallel to the temperature gradient. Their results show that natural convection is suppressed with an imposed magnetic field, and the magnetic damping effect increases with an increase in the applied field strength. Recently, Kolsi et al. [17] carried out a numerical study of natural convection in a differentially heated cubic cavity for $\mathrm{Pr} = 0.045$ under the presence of an external magnetic field orthogonal to the isothermal walls. They observed a damping and laminarization effects of the external magnetic field, and an organization of the central three-dimensional motion.

In this article, the combined effects of wall electrical conductivity and magnetic field orientation on the flow and thermal structure are numerically investigated, and the results are discussed within the context of Bridgman crystal growth. Section 2 presents the mathematical formulation. Section 3 discusses the numerical method and techniques, which have been used for the computation. Section 4 presents the grid independence study. Section 5 presents the results and the comparison between our predictions and the experimental results of Hof et al. [14]. Finally, a conclusion is given.

2. GEOMETRY AND MATHEMATICAL MODEL

The chosen geometry is that considered by Hof et al. [14] in their experimental study. The schematic view of the problem is shown in Figure 1. The liquid gallium sample whose Prandtl number is equal to 0.019 is enclosed in a rectangular enclosure of relative dimensions $L = 5.0 \times W = 1.3 \times H = 1.0$, and subject to a controlled horizontal temperature difference, which drives the convective flow. The left wall is kept at a local cold temperature T_c, and the right wall is maintained at a local hot temperature T_h. The other walls are adiabatic. A uniform magnetic field is applied in two directions, namely longitudinal (the magnetic field Bx is parallel to the temperature gradient), and vertical (the magnetic field By is parallel to gravity).

The interaction between the magnetic field and convective flow involves an induced electric current $\vec{j}$,

$$\vec{j} = \sigma\left[-\vec{\nabla}\varphi + \vec{V} \wedge \vec{B}\right] \tag{1}$$

The divergence of Ohm's law $\nabla \cdot \vec{j} = 0$, produces the equation of the electric potential φ.

$$\nabla^2\varphi = \vec{\nabla}\left(\vec{V} \wedge \vec{e}_B\right) \tag{2}$$

By neglecting the induced magnetic field, the dissipation and Joule heating, and using $L, \nu/L$, L^2/ν, $\rho_0(\nu/L)^2$, νB_0, and $(T_h\text{-}T_c)$ as typical scales for lengths, velocities, time, pressure, potential, and temperature, respectively, the dimensionless

governing equations for the conservation of mass, momentum, and energy with the Bousinesq approximation, together with appropriate initial and boundary conditions in the Cartesian coordinates system (x, y, z), are written in dimensionless form, as follows.

$$\nabla \cdot \vec{V} = 0 \tag{3}$$

$$\frac{\partial \vec{V}}{\partial t} + \left(\vec{V} \cdot \nabla\right)\vec{V} = -\nabla p + \nabla^2 \vec{V} - \mathrm{Gr} T \vec{g} + \mathrm{Ha}^2 \left[\left(\vec{V} \times \vec{B}\right) \times \vec{B}\right] \tag{4}$$

$$\frac{\partial T}{\partial t} + \vec{V} \cdot \nabla T = \frac{1}{\mathrm{Pr}} \nabla^2 T \tag{5}$$

where $\mathrm{Gr} = g\beta(T_h - T_c)L^3/\nu^2$ is the Grashof number, $\mathrm{Ha} = B_0 L\sqrt{\sigma/\mu}$ is the Hartmann number, and $\mathrm{Pr} = \nu/\alpha$ is the Prandtl number.

The initial conditions impose that the fluid is at rest and that the temperature distribution is zero, and that the electric potential is zero everywhere in the rectangular enclosure. Thus, at $t = 0$, we have: $u = v = w = T = \varphi = 0$.

The boundary conditions of the dimensionless quantities (u, v, w, and T) are

$$\text{At} \quad x = 0, \quad u = v = w = 0, \quad T = 0 \tag{6a}$$

$$\text{At} \quad x = 5, \quad u = v = w = 0 \quad T = 1 \tag{6b}$$

$$\text{At } y = 0, \quad u = v = w = 0 \quad \frac{\partial T}{\partial y} = 0 \tag{6c}$$

$$\text{At } y = 1, \quad u = v = w = 0 \quad \frac{\partial T}{\partial y} = 0 \tag{6d}$$

$$\text{At } z = 0, \quad u = v = w = 0 \quad \frac{\partial T}{\partial z} = 0 \tag{6e}$$

$$\text{At } z = 1.3, \quad u = v = w = 0 \quad \frac{\partial T}{\partial z} = 0 \tag{6f}$$

In this study, we have considered several cases of the boundary conditions for the electrical potential φ, for electrically insulating walls, $\partial\varphi/\partial n = 0$, and for a perfectly electrically conducting wall, $\varphi = 0$.

3. NUMERICAL METHOD

Governing equations (2)–(5), with the associated boundary conditions, were solved using a finite-volume method, as described by Patankar [18]. The components of the velocity (u, v, and w) are stored at the staggered locations, and the scalars

quantities (P, T, and φ) are stored in the center of these volumes. The numerical procedure called SIMPLER [18] is used to handle the pressure-velocity coupling. The second-order accurate central difference scheme is used to discretize the convection and diffusion terms. This approach was utilized recently by Bessaih and Bouabdallah [19] for predicting the onset of oscillatory convection in a rectangular cavity filled with a pure liquid metal during the phase change. Temporal discretisation is first order accurate and fully implicit [19]. Finally, the discretized algebraic equations are solved by the line-by-line tridiagonal matrix algorithm (TDMA). Convergence at a given time step is declared when the maximum relative change between two consecutive iteration levels fell below than 10^{-4}, for u, v, w, and T. At this stage, the steady state solution is obtained. A parallel test was made to guarantee that the energy balance between the hot and cold walls is less than a prescribed accuracy value, i.e., 0.2%. Calculations were carried out on a PC with CPU 3 GHz; thus, the average computing time for a typical case was approximately 5 hours.

4. GRID INDEPENDENCE STUDY

The increments Δx, Δy, and Δz of the grid used are not regular. They have been chosen according to geometric progressions of ratio 1.07, which permits a grid refinement near the walls. In order to examine the effect of the grid on the numerical solution, a number of grid sizes have been investigated for grid independence study: $62 \times 32 \times 42$ nodes, $92 \times 42 \times 52$ nodes, and $100 \times 50 \times 60$ nodes. By increasing the grid size from a $92 \times 42 \times 52$ nodes to $100 \times 50 \times 60$ nodes, a change of less than 2% in computed values was observed in (seen in Figure 2). Therefore, in order to capture the Hartmann and side layers, the grid used has $92 \times 42 \times 52$ nodes and was chosen after performing grid independence tests, since it is considered to have the best compromise between the computing time and the sufficient resolution in calculations.

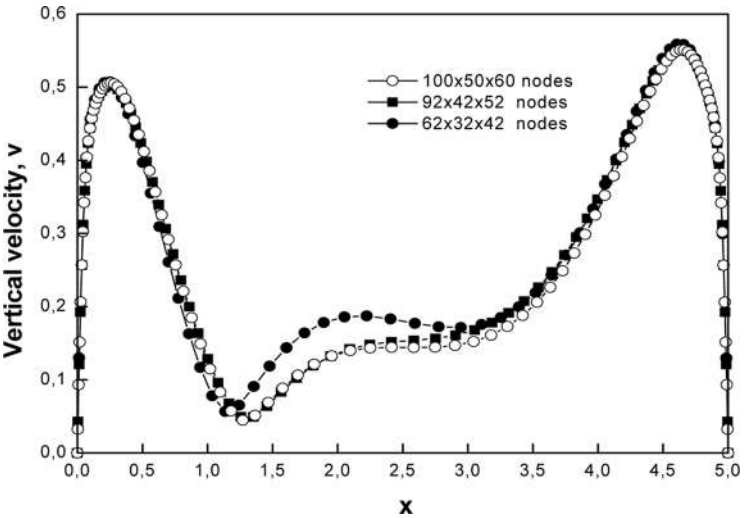

Figure 2. Profiles of the dimensionless vertical velocity v with x for different grids, at $y = H/2$ and $z = W/2$ ($\mathrm{Gr} = 3.75 \times 10^4$).

5. RESULTS AND DISCUSSION

5.1. Flow Structure

Figures 3–5 show the velocity vectors for $Ha = 0$ and $Ha = 50$ for the longitudinal field and $Ha = 50$ for the vertical field, respectively. Figure 3*a*, 4*a*, and 5*a* show the perspective views of velocity vectors, respectively, for six transverse sections of the cavity: $x = 0.22$; $x = 0.89$; $x = 2.83$; $x = 4.35$, and $x = 4.86$. The same scale was

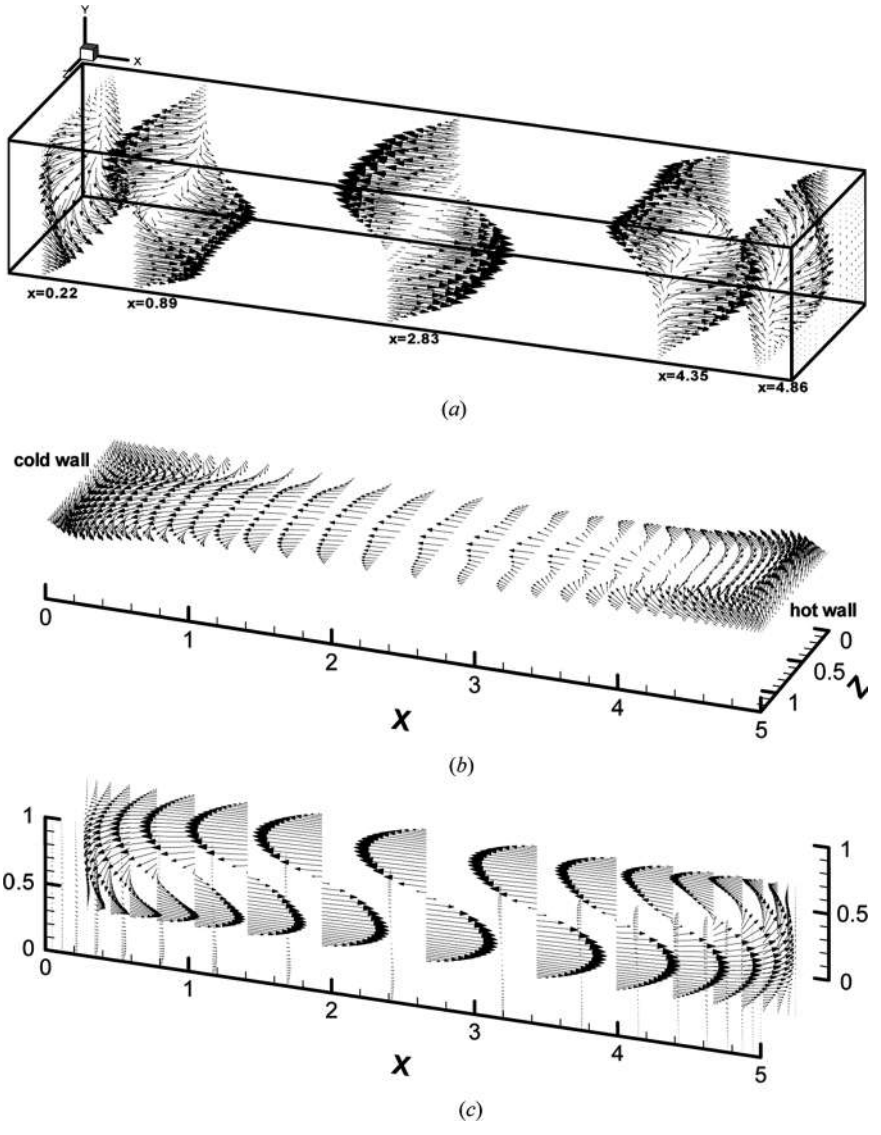

Figure 3. Velocity-vector for $Gr = 3.75 \times 10^4$ and $Ha = 0$ (without magnetic field). (*a*) In the enclosure, (*b*) in the *X*-*Z* plane, and (*c*) in the *X*-*Y* plane.

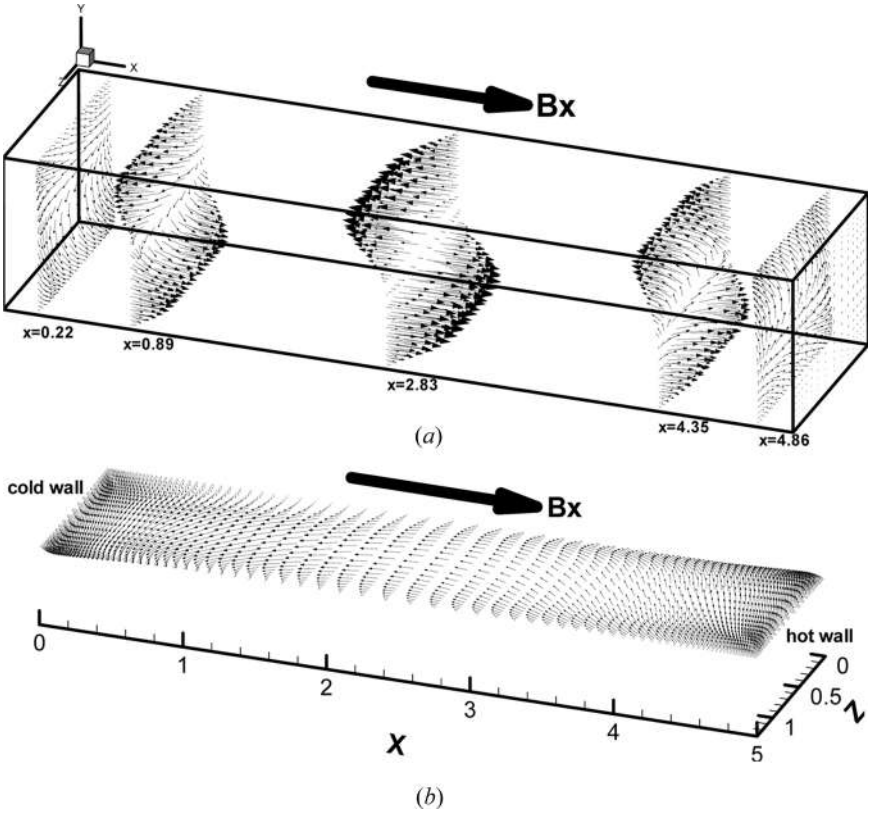

Figure 4. Velocity-vector for $Gr = 3.75 \times 10^4$ and $Ha = 50$ (with magnetic field Bx). (*a*) In the enclosure and (*b*) in the X-Z plane.

chosen for all predictions. It is clear from these figures that the velocity field is strongly reduced in the presence of a magnetic field. In the absence of the magnetic field $Ha = 0$, the velocity vectors over the hot wall are directed upward, those near the cold wall are directed downward, and those near the side walls are larger than those in the central region. They show a very important three-dimensional unicellular convective circulation, which is clearly reduced if a magnetic field is applied longitudinally (Figure 4) and reduced most strongly to a two-dimensional convective circulation if a magnetic field is applied vertically (Figure 5). At $Ha = 50$, if the magnetic field is oriented vertically, the magnitude of velocity vectors are almost equal everywhere. Figure 3*c* shows a basic unicellular circulation from the cold wall toward the hot wall in the lower part of the enclosure and from the hot wall toward the cold wall in the upper part of the enclosure. The flow exhibited Centro symmetry with respect to the almost diagonal straight line. On each side of the diagonal, a parabolic velocity profile is shown in which the maximum velocity increases away from the isothermal end walls and decreases closer to them. This profile locates the vortex core at the middle of the cavity. In this study, the comportment of velocity profiles is in good agreement with that found by Aleksandrova and Molokov [8]. Vectors velocity have their maxima near the middle of the cavity where the flow is

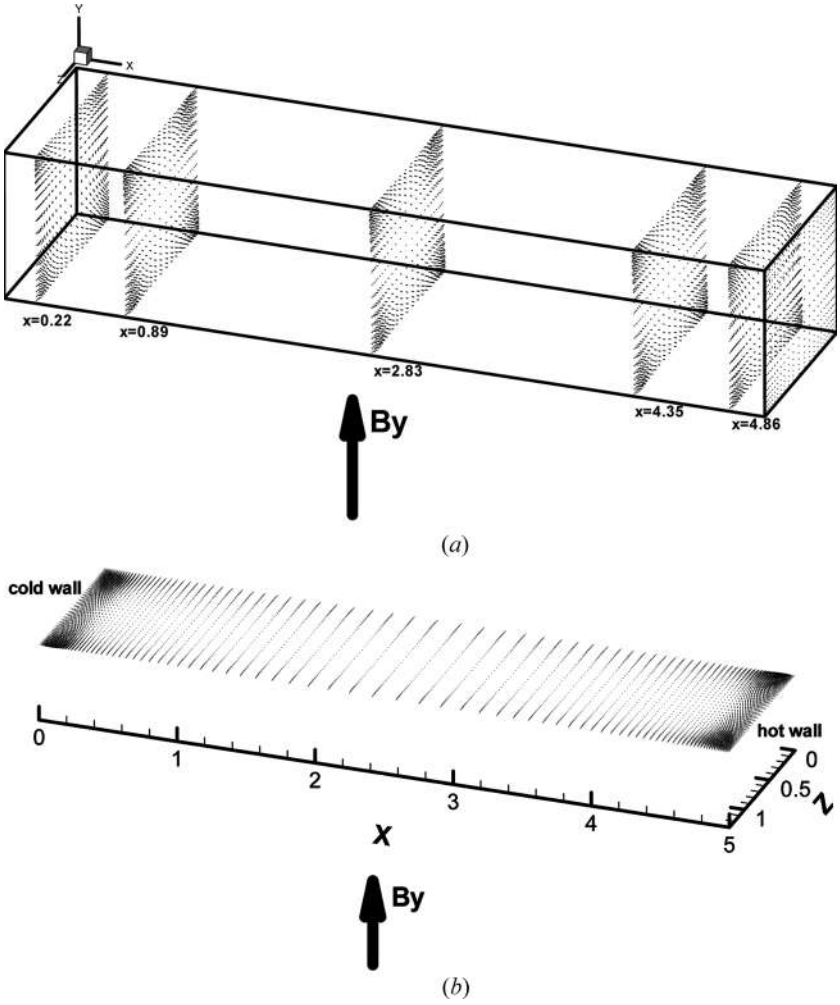

Figure 5. Velocity-vector for $Gr = 3.75 \times 10^4$ and $Ha = 50$ (with magnetic field By). (a) In the enclosure and (b) in the X-Z plane.

fully developed, and the velocity is significantly reduced closer to the ends of the cavity where the flow turn occurs.

Figures 6*a* and 6*b* illustrate the variation of the w-component of velocity in the x-y plane at $z = 0.25$ for two directions of the magnetic field (Bx and By). Comparison between these two figures shows that a remarkable modification of the structure of the flow exists when the direction of magnetic field changes. With a vertically magnetic field, the w-velocity component decreases faster in the core region and two almost antisymmetrical maxima of velocity are apparent near the vertical side walls. However, with the longitudinally magnetic field, two recirculations appear in the enclosure and the magnitude of velocity in the core is still important. In order to obtain the similar effect of the vertical magnetic field ($Ha = 50$) on the flow, a

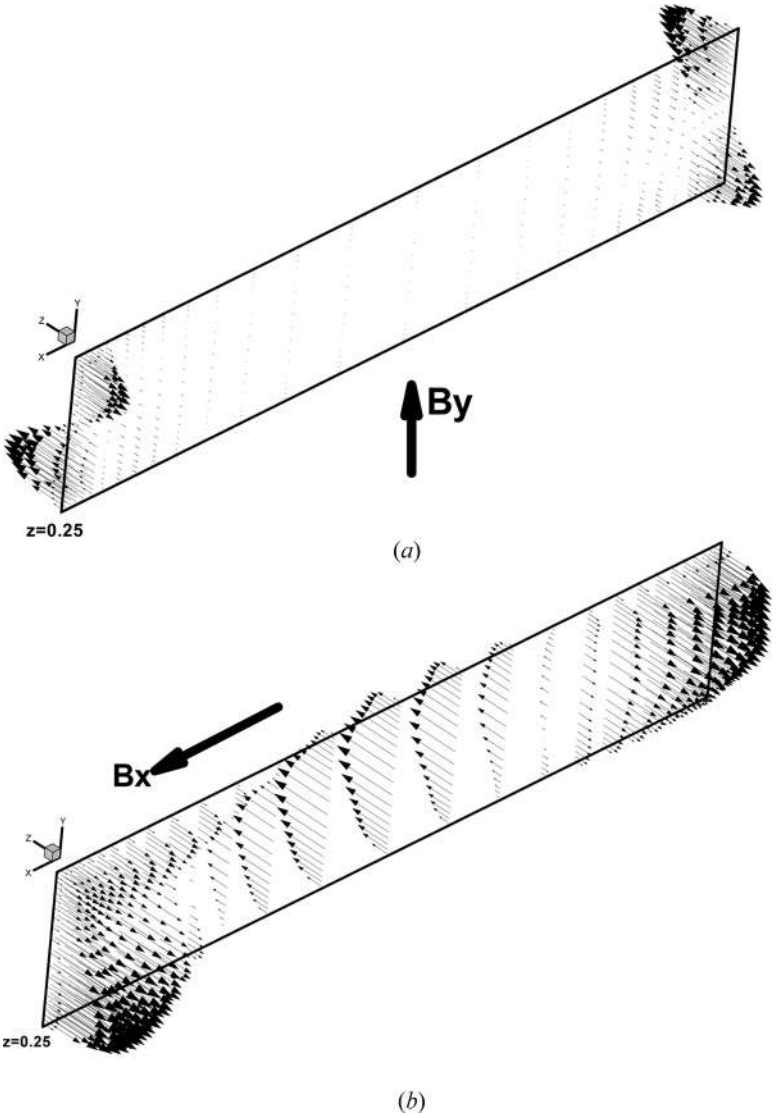

Figure 6. Velocity-vector of the w-velocity for $\mathrm{Gr} = 3.75 \times 10^4$ and $\mathrm{Ha} = 50$ (with magnetic field). (*a*) The magnetic field *By* is oriented in the *y*-direction and (*b*) the magnetic field *Bx* is oriented in the *x*-direction.

greater value of Ha (>50) must be used in the longitudinal direction of magnetic field. This is in good agreement with results found by Benhadid and Henry [2], who show that the damping effect for $\mathrm{Ha} = 200$ in the longitudinal direction was similar to that for $\mathrm{Ha} = 100$ in the vertical direction in the case of cavity with an aspect ratio $4 \times 1 \times 1$.

Figure 7 presents some particle tracks on the enclosure for various Hartmann numbers. In the absence of the magnetic field, the flow pattern shows the irregular three-dimensional flow due to pure buoyancy convection ($\mathrm{Ha} = 0$) (Figure 7*a*). By

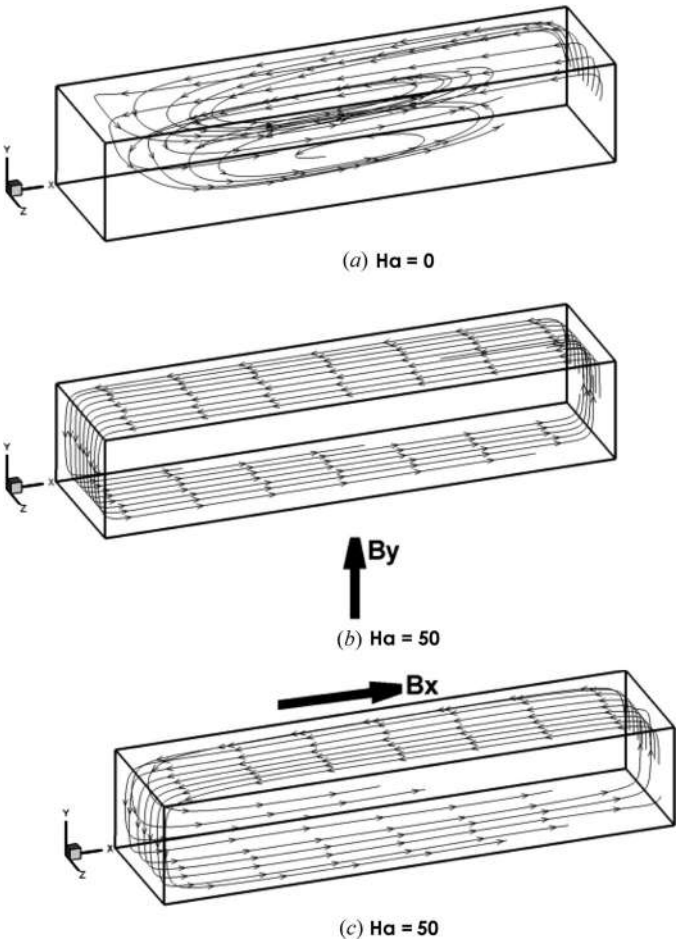

Figure 7. Some particle tracks for $Gr = 3.75 \times 10^4$ (with and without magnetic field). (*a*) Without magnetic field; (*b*) the magnetic field *By* is oriented in the *y*-direction; and (*c*) the magnetic field *Bx* is oriented in the *x*-direction.

increasing the Hartmann number Ha, the three-dimensional flow becomes more organized; in effect, for $Ha = 50$ the flow is more regular, while the tangential growth flow near the lateral walls is approximately insensitive to the direction of the magnetic field. Therefore, the effect of the direction of the magnetic field on the three-dimensional flow is essentially in the center of the enclosure.

5.2. Potential and Electrical Structures

Figure 8*a* presents the electric potential field at $Ha = 50$ for the longitudinal magnetic field. In this case, the directly induced electric current comes principally from interaction with the vertical velocity component, mainly near the sidewalls and the end walls. The potential is antisymmetric with respect to the middle *x*-*y* plane; it is also of opposite signs in the right and left parts of the enclosure. Figures 8*b* and 9 present,

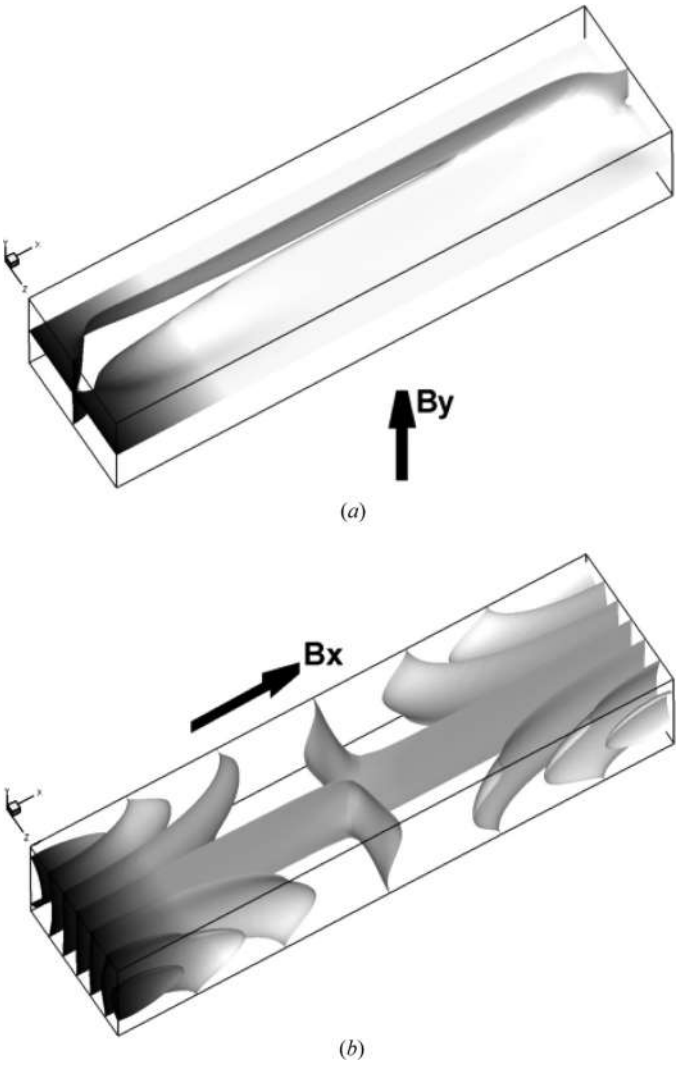

Figure 8. Iso-surfaces of electric potential for $\mathrm{Gr} = 3.75 \times 10^4$ and $\mathrm{Ha} = 50$. (*a*) The magnetic field *By* is oriented in the *y*-direction and (*b*) the magnetic field *Bx* is oriented in the *x*-direction.

respectively, the perspective of the electric potential and current density vector in some planes of x constant for the vertical magnetic field. There is a rotating current circulation created by vertical gradients of electric potential, and this potential also creates horizontal currents near the corners. A very good similarity can be observed with the results of Benhadid and Henry [2] and Aleksandrova and Molokov [8].

5.3. Thermal Structure

The isotherms for the enclosure without a magnetic field are shown in Figure 10*a*. A strong convection is indicated by distorted isotherms within the enclosure.

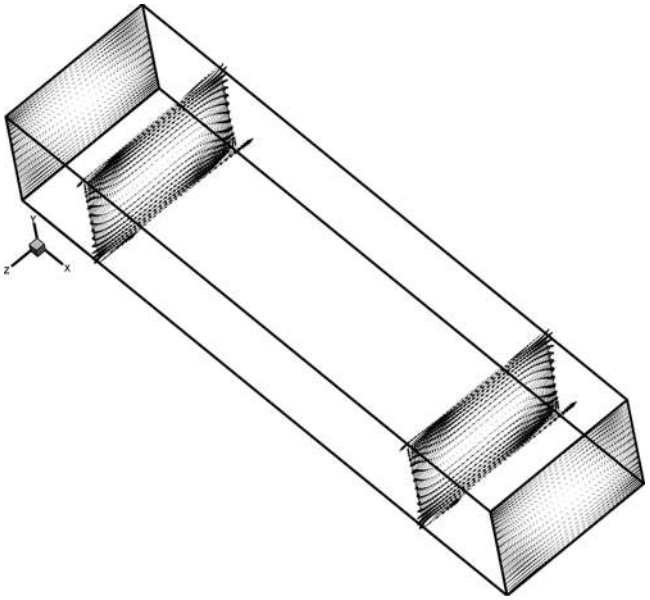

Figure 9. Electric currents for $Gr = 3.75 \times 10^4$ and $Ha = 50$ (here, the magnetic field By is oriented in the y-direction).

With application of the magnetic field, thermal stratification in the core of the enclosure is destroyed and the isotherms become parallel to the vertical walls, indicating the dominance of the conduction regime, as shown in Figures 10*b* and 10*c*. Also, isotherms in the vertically oriented magnetic field case are the least distorted, implying reduced convective heat transfer, as compared to the longitudinally orientation.

5.4. Local and Average Nusselt Numbers

The iso-contours of the local Nusselt number on the hot wall of the enclosure represented in Figure 11 show that the variations according to y-direction are attenuated in the presence of the magnetic field. This involves an important two-dimensionalization of heat transfer. At $Ha = 0$ (Figure 11*a*), the maximum value of the local Nusselt number (defined as $Nu = -\partial T/\partial x$ is 1.80, decreases to 1.4 for $Ha = 45$ when the magnetic field is longitudinal (Figure 11*b*), and to 1.0 for $Ha = 45$ when the magnetic field is vertical (Figure 11*c*), which signifies that the vertical magnetic field reduces the heat transfer more than the longitudinal one, and is the same tendency as the experimental observation [16]. This result is in good agreement to that found by Kolsi et al. [17]. The iso-contours on the wall compare favorably with experimental measurements [20].

When the magnetic field is oriented vertically, Figures 12*a*–12*c* show the variations of u_{max}, v_{max}, and w_{max} and Figure 13 illustrates the average Nusselt number Nu_{avg} with the Hartmann number Ha for four cases considered here. Case 1: all

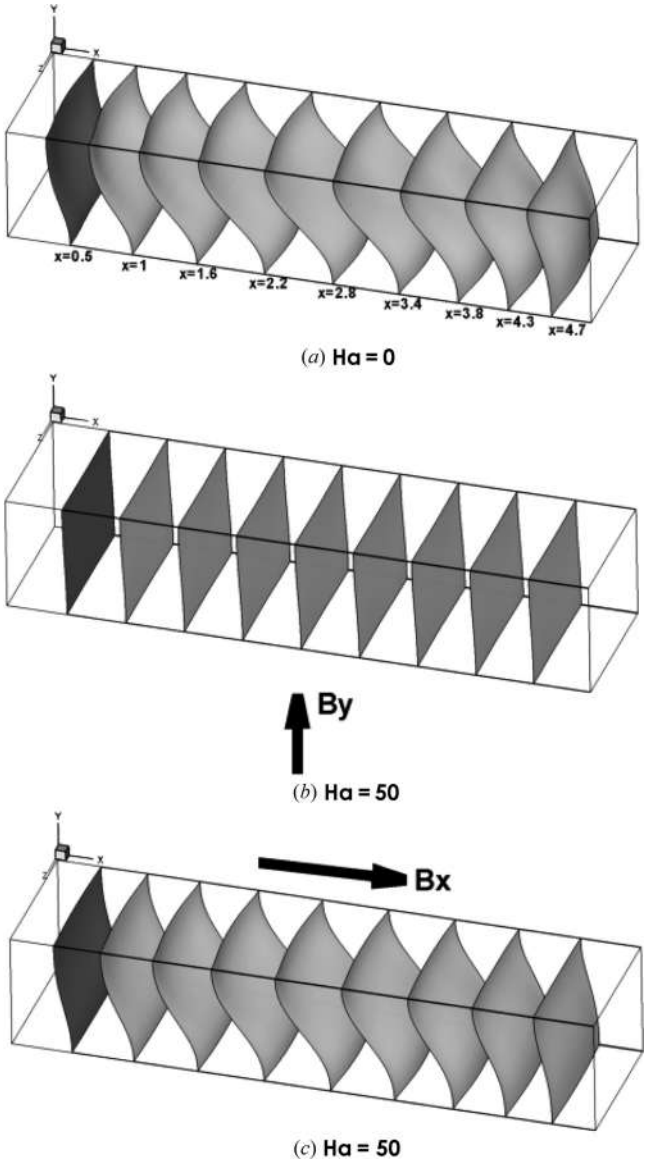

Figure 10. Iso-surfaces of temperature for $\mathrm{Gr} = 3.75 \times 10^4$ (with and without magnetic field). (*a*) Without magnetic field, (*b*) the magnetic field *By* is oriented in the *y*-direction, and (*c*) the magnetic field *Bx* is oriented in the *x*-direction.

walls are electrically insulating; case 2: only the vertical walls ($x = 0$ and $x = 5$) are electrically conducting; case 3: only the horizontal walls ($y = 0$ and $y = 1$) are electrically conducting; and case 4: only the frontal walls ($z = 0$ and $z = 1.3$) are electrically conducting. We can see from Figures 12 and 13 that the convection is best damped when the frontal walls are electrically conducting ($z = 0$ and $z = 1.3$). This is because

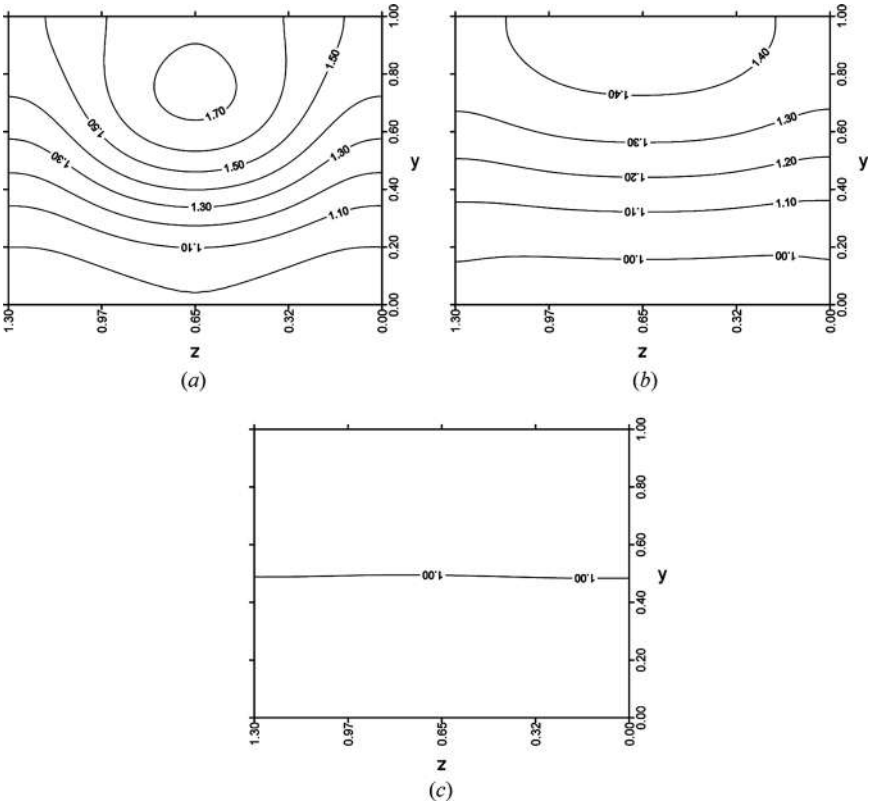

Figure 11. Iso-contours of the local Nusselt number on the hot wall for $Gr = 3.75 \times 10^4$. (*a*) Without magnetic field, $Ha = 0$; (*b*) the magnetic field *Bx* is oriented in the *x*-direction, $Ha = 45$; and (*c*) the magnetic field *By* is oriented in the y-direction, $Ha = 45$.

the wall electrical conducting leads to a lower source or to higher sink terms in the momentum equations, depending on the flow direction, i.e., to an overall damping of the flow. For example, at $Ha = 10$ the average Nusselt number is 1.45 for case 1 and 1.40 for case 4.

Concerning the effect of the electroconductivities of the wall, the values of the average Nusselt number obtained between the present work and the numerical results of Tagawa and Ozoe [21] are shown in Table 1. A small difference between these values is obtained.

5.5. Comparison between Experimental and Numerical Results

A quantitative comparison between experimental results obtained by Hof et al. [14] and our numerical simulations was performed, using the determination of the vertical temperature difference $\overline{\Delta_{mid}} = (\Delta_{mid}(Ha)/\Delta_{mid}(Ha = 0))$ with $\Delta_{mid} = T2 - T5$, and the longitudinal temperature difference $\overline{\Delta_{long}} = (\Delta_{long}(Ha)/\Delta_{long}(Ha = 0))$ with $\Delta_{long} = T3 - T1$ (Figure 14*a*) for two magnetic fields orientations: vertical and

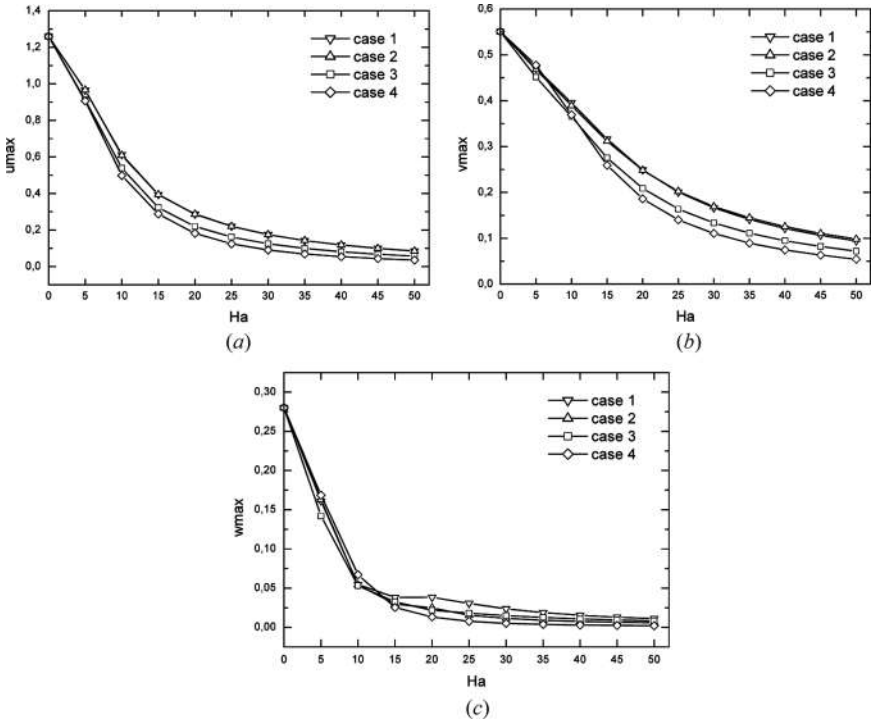

Figure 12. Variation of u_{max}, v_{max}, and w_{max} with the Hartmann number at $Gr = 3.75 \times 10^4$ for different cases. Case 1: all walls are electrically conducting; case 2: only the vertical walls are electrically conducting; case 3: only the horizontal walls are electrically conducting; and case 4: only the frontal walls are electrically conducting. (*a*) u_{max}; (*b*) v_{max}; and (*c*) w_{max}.

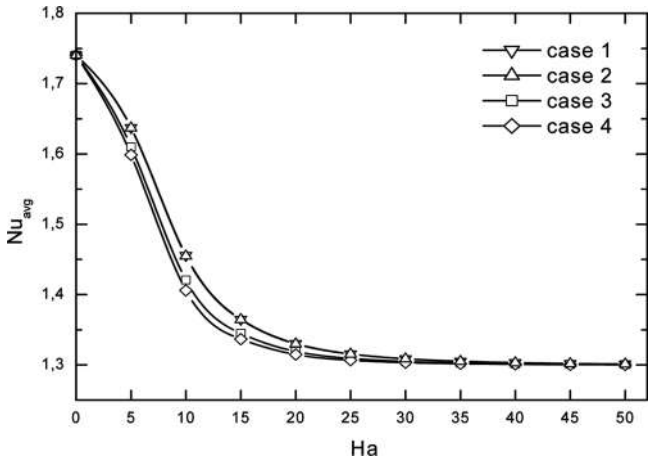

Figure 13. Variation of the average Nusselt number Nu_{avg} with the Hartmann number Ha for different cases. Case 1: all walls are electrically conducting; case 2: only the vertical walls are electrically conducting; case 3: only the horizontal walls are electrically conducting; and case 4: only the frontal walls are electrically conducting; at $Gr = 3.75 \times 10^4$.

Table 1. Comparison between our numerical results and those of Tagawa and Ozoe [21]

	Ra	Pr	Ha	Nu_{avg}
Present work	10^5	0.025	100	1.120
Tagawa and Ozoe [21]	10^5	0.025	100	1.235

Here, the magnetic field is oriented in the x-direction and all walls are perfectly electrically conducting. Ra is the Rayleigh number.

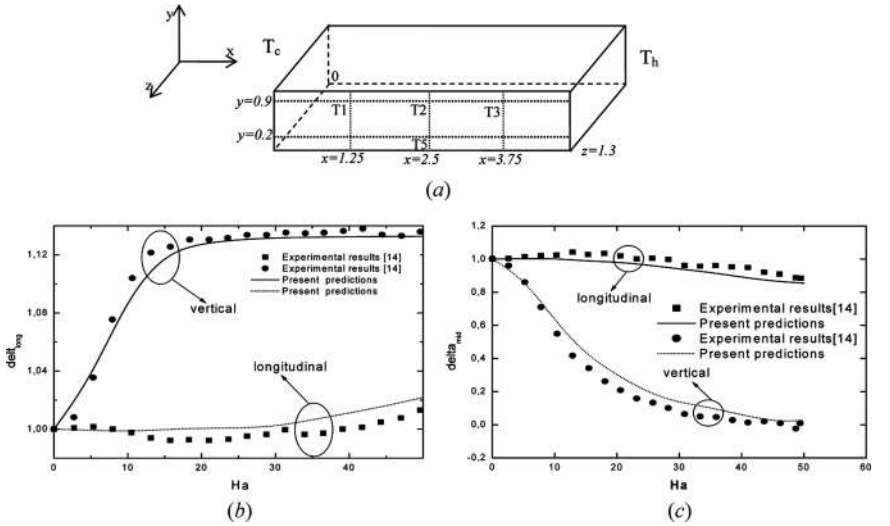

Figure 14. (*a*) Positions of the thermocouple probes in the temperature difference, used in the experimental study of Juel et al. [14]; (*b*) comparison between our predictions and experimental results [14] of the variation of the vertical temperature difference with the Hartmann number ($Gr = 3.75 \times 10^4$); and (*c*) comparison between our predictions and experimental results [14] of the variation of the longitudinal temperature difference with the Hartmann number ($Gr = 3.75 \times 10^4$).

longitudinal, with $Gr = 3.75 \cdot 10^4$ and $Pr = 0.019$. As shown in Figures 14*b* and 14*c*, a good agreement between the experimental data and our numerical results is obtained.

6. CONCLUSION

A three-dimensional numerical study of a low-Prandtl number fluid flow inside a rectangular enclosure under an external magnetic field in either the vertical or longitudinal direction has been carried out. The geometry considered here is related to crystal growth by a horizontal Bridgman configuration. The finite-volume method has been used to discretize the mathematical model. The main results are as follows.

- A good agreement between numerical and experimental data was obtained during code validation.

- An increase in the strength of the magnetic field causes the flow to evolve both in magnitude and in form.
- The intensity of the flow is reduced in two cases, so a regularization of the three-dimensional spiraling flow is observed in the core of the enclosure.
- In the absence of the magnetic field, the flow pattern shows the irregular three-dimensional flow due to pure buoyancy convection.
- In the presence of the magnetic field, the flow is more regular.
- The decrease of the flow is stronger for the vertical field orientation (transverse to the temperature gradient) and weaker for the longitudinal one (aligned with the temperature gradient).
- With the application of the magnetic field, thermal stratification in the core of the enclosure is destroyed and the isotherms become parallel to the vertical walls.
- The convection is best damped when the frontal walls are electrically conducting.

In conclusion, the results indicate that the flow can be controlled via a good choice of strength and direction of the magnetic field, as well as of the electric conductivity of the enclosure walls.

REFERENCES

1. T. Tagawa and H. Ozoe, Enhancement of Heat Transfer Rate by Application of a Static Magnetic Field During Natural Convection of Liquid Metal in a Cube, *ASME J. Heat Transfer*, vol. 119, pp. 265–271, 1997.
2. H. Benhadid and D. Henry, Numerical Study of Convection in the Horizontal Bridgman Configuration under the Action of a Constant Magnetic Field, Part 2, Three-Dimensional Flow, *J. Fluid Mech.*, vol. 333, pp. 57–83, 1997.
3. A. F. Emery and J. W. Lee, The Effects of Property Variations on Natural Convection in a Square Enclosure, *ASME J. Heat Transfer*, vol. 121, pp. 57–62, 1999.
4. R. Bessaih, M. Kadja, and Ph. Marty, Effect of Wall Electrical Conductivity and Magnetic Field Orientation on Liquid Metal Flow in a Geometry Similar to the Horizontal Bridgman Configuration for Crystal Growth, *Inter. J. Heat and Mass Transfer*, vol. 42, pp. 4345–4362, 1999.
5. S. Saravanan and P. Kandaswamy, Natural Convection in Low-Prandtl Number Fluids with a Vertical Magnetic Field, *ASME J. Heat Transfer*, vol. 122, pp. 602–606, 2000.
6. S. Arcidiacono, I. Di Piazza, and M. Ciofalo, Low-Prandtl Number Natural Convection in Volumetrically Heated Rectangular Enclosures, II, Square Cavity, $AR = 1$, *Inter. J. Heat and Mass Transfer*, vol. 44, pp. 537–550, 2001.
7. S. Arcidiacono and M. Ciofalo, Low-Prandtl Number Natural Convection in Volumetrically Heated Rectangular Enclosures, III, Shallow Cavity, $AR = 0.25$, *Inter. J. Heat and Mass Transfer*, vol. 44, pp. 3053–3065, 2001.
8. S. Aleksandrova and S. Molokov, Three-Dimensional Buoyant Convection in a Rectangular Cavity with Differentially Heated Walls in a Strong Magnetic Field, *Fluid Dyn. Res.*, vol. 35, pp. 37–66, 2004.
9. M. S. Krakov and I. V. Nikiforov, To the Influence of Uniform Magnetic Field on Thermomagnetic Convection in Square Cavity, *J. Magnetism and Magnetic Materials*, vol. 252, pp. 209–211, 2002.
10. M. S. Krakov, I. V. Nikiforov, and A. G. Reks, Influence of the Uniform Magnetic Field on Natural Convection in Cubic Enclosure: Experiment and Numerical Simulation, *J. Magnetism and Magnetic Materials*, vol. 289, pp. 272–274, 2005.

11. I. E. Sarris, S. C. Kakarantzas, A. P. Grecos, and N. S. Vlachos, MHD Natural Convection in a Laterally and Volumetrically Heated Square Cavity, *Inter. J. Heat and Mass Transfer*, vol. 48, pp. 3443–3453, 2005.
12. T. Sophy, H. Sadat, and L. Ghahoué, Convection Thermomagnétique dans une Cavité Différentiellement Chauffée, *Inter. Commun. Heat and Mass Transfer*, vol. 32, pp. 923–930, 2005.
13. M. Kaneda, T. Tagawa, and H. Ozoe, Natural Convection of Liquid Metal under a Uniform Magnetic Field with an Electric Current Supplied from Outside, *Experi. Thermal and Fluid Sci*., vol. 30, pp. 243–252, 2006.
14. B. Hof, A. Juel, and T. Mullin, Magnetohydrodynamic Damping of Convective Flows in Molten Gallium, *J. Fluid Mechanics*, vol. 482, pp. 163–179, 2003.
15. B. Hof, A. Juel, and T. Mullin, Magnetohydrodynamic Damping of Oscillations in Low-Prandtl-Number Convection, *J. Fluid Mech*., vol. 545, pp. 193–201, 2005.
16. B. Xu, B. Q. Li, and D. E. Stock, An Experimental Study of Thermally Induced Convection of Molten Gallium in Magnetic Fields, *Inter. J. Heat and Mass Transfer*, vol. 42, pp. 2009–2019, 2006.
17. L. Kolsi, A. Abidi, M. N. Borjini, N. Daous, and H. Ben Aïssa, Effect of an External Magnetic Field on the 3-D Unsteady Natural Convection in a Cubical Enclosure, *Numer. Heat Transfer A*, vol. 51, pp.1003–1021, 2007.
18. S. V. Patankar, *Numerical Heat Transfer and Fluid Flow*, Hemisphere, Washington, D.C., 1980.
19. R. Bessaïh and S. Bouabdallah, Numerical Study of Oscillatory Natural Convection during Solidification of a Liquid Metal in a Rectangular Enclosure with and without Magnetic Field, *Numer. Heat Transfer A*, vol. 54, pp. 331–345, 2008.
20. M. G. Braunsfurth, A. C. Skeldon, A. Juel, T. Mullin, and D. S. Riley, Free Convection in Liquid Gallium, *J. Fluid Mech*., vol. 342, pp. 295–314, 1997.
21. T. Tagawa and H. Ozoe, The Natural Convection of Liquid Metal in a Cubical Enclosure with Various Electro-Conductivities of the Wall under the Magnetic Field, *Inter. J. Heat and Mass Transfer*, vol. 41, no. 13, pp. 1917–1928, 1998.